JOURNAL OF SOLID STATE CHEMISTRY 39, 56–74 (1981)

Chevrel Phases: An Analysis of Their Metal–Metal Bonding and Crystal Chemistry

JOHN D. CORBETT

Ames Laboratory–DOE and Department of Chemistry, Iowa State University, Ames, Iowa 50011*

Received December 8, 1980; in final form March 2, 1981

A useful measure of the total Mo–Mo bonding in diverse phases containing Mo_6Y_8-type clusters (Y = S, Se, Cl, Br) is given by the Pauling bond order sum per electron (PBO/e). These fall into two classes: (a) strongly bonded examples with PBO/e values near 1.00 which contain either discrete clusters with extra outer (exo) atoms or infinite confacial clusters, and (b) the rhombohedral Mo_6Ch_8 and $M_xMo_6Ch_8$ Chevrel phases with reduced PBO/e values of 0.72–0.84 in which face-capping chalcogenide (Ch) must also fill exo positions. The matrix effect in the latter which is responsible for the reduced bond orders arises from a combination of particularly strong Mo–Ch intercluster bonds and closed-shell Ch–Ch repulsions [3.31 Å (S), 3.38 Å (Se)], which force an elongation of the Mo_6 trigonal antiprism and reduce the Mo–Mo bonding. There is no distinction between sulfide and selenide Chevrel phases in the degree of total Mo–Mo bonding as expressed in bond orders. Changes in the structure on reduction are analyzed; the major effects come from loosening of the intercluster Mo–Ch bonding and thence a decreased distortion (matrix effect) together with a flexing of the Mo_6Ch_8 host according to the size and charge of M. Distance considerations indicate substantial covalency between some M and $Ch2$, especially Pb and Ag, while cell volumes and Mo–$Ch2$ distances suggest significant constriction occurs in phases with higher charged M, possibly owing to compression by the host lattice and coulombic contributions to binding. Evidence for Mo–M bonding with M = Fe, Co, Ni is also noted. Intercluster interactions and Mo–Mo bonding in $Mo_6S_6Br_2$ and in the mixed Mo_6Ch_8–Mo_nCh_m (n = 9,12) cluster phases are quite consistent with those in the Chevrel phases, the total Mo–Mo bonding per electron increasing with cluster condensation owing principally to reduce Ch–Ch repulsions.

Introduction

Some degree of metal–metal bonding is a feature of a wide variety of inorganic compounds. Recently some systematics relating metal–metal bonding in different structures and with a variety of metals have been developed in terms of metallic bond orders (*1*). In a good fraction of the examples the magnitude of the metal–metal interactions are found to be significantly limited by matrix or steric effects generated by nonmetal packing, the effect on metal–metal bond order without exception being plausible and consistent. Most importantly, anion–anion repulsions (matrix effects) in a considerable number of metal-rich halides and chalcogenides are found to be sufficiently small—within M_6X_8-type cluster groups, for example—that the total amount of metal–metal

* Operated for the U.S. Department of Energy by Iowa State University under Contract W-7405-Eng-82. This research was supported by the Assistant Secretary for Energy Research, Office of Basic Energy Sciences, WPAS-KC-02-03.

0022-4596/81/100056-19$02.00/0

bonding is much the same as the metal when considered in terms of empirical Pauling (*2*) bond order equation (1)

$$D_n = D_1 - 0.60 \log n \qquad (1)$$

and the number of electrons involved. Here the value of D_1—twice the "single-bond metallic radius"—is based on the known structure and valence of the metal. For example, the 12-coordinate separation in molybdenum metal is 2.800 Å (*3*) and with six valence electrons the single-bond distance is defined as 2.800 + 0.6 log ($\frac{6}{12}$) = 2.619 Å. Starting with such metal-based calibrations the sum of metal–metal bond orders over all independent metal–metal distances divided by the number of electron pairs available for bonding has been calculated for many metal-rich compounds of transition groups III–VI. The quotient is found to be remarkably close to 1.0 for 30 or so examples which are also logically free of matrix effects, principally those containing discrete or extended clusters (*1*). Implicit in the success of this approach is that nonmetal participation in bonding (mixing in the metal valence or conduction band) is not important in determining metal–metal distances and neither are the geometry of the metal structure or the degree of delocalization.

A prevalent feature of reduced molybdenum chemistry is the occurrence of strongly bonded M_6X_8-type clusters, Mo_6 octahedra with typical nearest neighbor distances of 2.6–2.8 Å, in which each face of the metal polyhedron is capped by a halide or chalcogenide atom. Ideally this generates a cube of nonmetal atoms with the molybdenum atoms on or near the cube faces. This construction is favorable for the development of strong Mo–Mo bonds without any matrix effect in the sense that the nonmetal separations in the ideal cluster are sufficiently great ($2^{1/2} d_{Mo-Mo}$) that they do not restrict the approach of the molybdenum atoms to one another, at least for nonmetals which are no larger than sulfur or chlorine. Application of this bond order equation to $(Mo_6Cl_8)Cl_4$ proceeds as follows: Recent data (*4*) indicate that each molybdenum has two pairs of neighbors at 2.604 and 2.608 Å, which, by the bond order equation, yield a sum of 2(1.06) + 2(1.04) = 4.20 for the bond order at molybdenum.[1] With four valence electrons per Mo atom left for metal–metal bonding the Pauling bond order per electron (PBO/*e*) is 4.20/4 = 1.05[2] or, in other words, very comparable to that in the metal itself in the distance sense (Eq. (1)) when the relative number of valence electrons is taken into account. Many other phases with well-separated Mo_6X_8 clusters behave similarly. On the other hand, the approach of metal atoms is definitely restricted by close nonmetal packing in, for example, the layered MoS_2 or the $W_6Cl_{12}^{6+}$ cluster (where chlorine now occurs on the edges of the previous cube), and the bond orders per electron are less than 0.5.

This impetus for the present study derived from the observation that the bond order sums per electron of 0.72–0.84 for the remarkable Chevrel phases $M_xMo_6Ch_8$, *Ch* = S, Se (*5–7*), are distinctly lower than those for other Mo_6X_8 clusters, the larger values in this range being associated with greater reduction (larger *x*) or higher valent *M*. Consideration of reasons for such a substantial difference in PBO/*e* values between the Chevrel phases and the other molybdenum clusters leads to the development of

[1] The only other significant Mo–Mo distances within the cluster are the 3.69-Å diagonals, for which $n = 0.02$.

[2] This procedure effectively counts each bond twice. Clearly the same result is obtained if the bond order sum over independent distances per cluster is divided by the number of electron pairs.

appreciable insight into the character and restrictions of bonding in the usual network structures exhibited by the Chevrel phases.

Results and Discussion

Bond Orders

Sums of Pauling bond orders per electron in compounds containing discrete Mo_6X_8 clusters are found to display an amazing consistency, viz., $(Mo_6Cl_8)Cl_4$, 1.05, $Hg(Mo_6Cl_8)Cl_6$ (*8*), 1.00; $(PyH^+)_3(Mo_6Cl_7S)Cl_6$ (*9*), 1.04;[3] $(Mo_6Cl_7Se)Cl_{6/2}$ (*10*), 1.01; $Mo_6S_6Cl_2 \cdot 6Py$ (*9*), 1.03; $(Mo_5Cl_8)Cl_5^{2-}$ [$(Mo_6Cl_8)Cl_6^{2-}$ missing one vertex (*11*)], 0.98. And to these may be added PBO/*e* values of 1.01 and 1.02 for the more reduced $Tl_2Mo_6Se_6$ and $In_2Mo_6Se_6$ (*12, 13*), infinite chain structures of confacial molybdenum octahedra ($Tl_2Fe_6Te_6$-type) in which the absence of a matrix effect is assured by minimum Se–Se separations of nearly 3.8 Å. The values calculated for other molybdenum compounds fall hand in hand with expectations regarding increased matrix effects (nonmetal repulsions) with more or larger anions, e.g., $(Mo_6Br_8)Br_4 \cdot (OH_2)_2$ (*14*), 0.94 (borderline); $(W_6Cl_{12})Cl_8$ (*15*), 0.44; and $3R$–MoS_2 (*16*), 0.38. For comparison with the Chevrel phases the 19- and 20-electron clusters $(Nb_6I_8)I_{6/2}$ (*17*) and $Cs(Nb_6I_8)I_{6/2}$ (*18*) evidently exhibit a modest matrix effect because of the larger iodine atoms; these require relatively longer Nb–Nb bonds and even with a larger D_1 (2.708 Å) correspond to PBO/*e* values of 0.80 and 0.81, respectively. The familiar edge-capped 6-12 clusters such as $Nb_6X_{12}^{n+}$ always contain relatively longer bonds and exhibit lower bond orders than the analogous Nb_6X_8 types unless X is small (O, F).

[3] *Py* = pyridine.

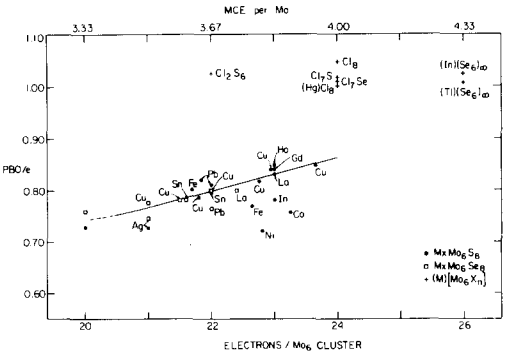

FIG. 1. The Pauling metal–metal bond order sum per electron (PBO/*e*) vs the metal-based electron count per Mo_6 cluster in Mo_6Y_8 clusters. Lower curve: Rhombohedral Chevrel phases $M_xMo_6Ch_8$ (●,S; □,Se); upper data: isolated and infinite confacial Mo_6 clusters labeled with counter cation and nonmetal content of cluster (+). References in text.

Figure 1 shows the Pauling bond orders per electron (PBO/*e*) for substantially all the rhombohedral molybdenum sulfide and selenide cluster phases as well as for the other isolated and extended clusters for which single-crystal structural data are available. (PBO/*e* for the missing Mo_6Te_8 is 0.65.) Unless otherwise noted the structural data for the former group were taken from the recent excellent review by Yvon (*6*). These PBO/*e* values are shown plotted against the total as well as the average number of metal-based cluster electrons MCE (*19*) (or valence electron concentration VEC (*6*)) (top of figure), these being based on the number of electrons remaining for metal–metal binding in the cluster after valence orbitals (valence bands) for the nonmetal have been filled. For the ternary Chevrel phases, an apparently well-accepted premise (*6, 20*) is that the cluster or MCE count includes the valence electrons donated to the Mo_6X_8 substrate (conduction band) by the third element, M. The oxidation states deduced for the M element are sensible but often based on unpublished data. These were taken as stated

except that the Ni^{+} listed for $Ni_{1.40}Mo_6S_8$ was considered unreasonable and Ni^{2+} was assumed, analogous to Co^{2+} and Fe^{2+}.[4] The deviation seen in Fig. 1 for phases involving these three ions and indium will receive further consideration later. But with these exceptions all of the bond order results are remarkably uniform, and in particular, there is no significant distinction between sulfides and selenides. In other words the total amount of bonding expressed as a bond order sum over all distances is a seemingly smooth function only of electron count. The source of the differences in bonding between the binary chalcides and the isolated Mo_6X_8-type clusters will be interpreted in terms of the substantial matrix effect which pertains to all the Chevrel phases and its change with electron count.

In the Chevrel phases the characteristic Mo–Mo distances over which the bond order sums are taken typically fall into three classes. Using the binary Mo_6S_8 as an example (*22*), there is a short 2.698-Å distance in the triangles generated by the $\bar{3}$ (crystallographic *c*) axis that define opposite faces of a trigonal antiprismatic (D_{3d}) cluster, an intermediate 2.862 Å between Mo atoms in different triangles, and, with half the frequency, a long intercluster distance of 3.084 Å which is so important for further delocalization. Changes in these on reduction of the sulfide cluster by added *M* are diverse: a small and fairly irregular change in the first, a substantial (7%) and fairly smooth decrease in the second, and a general increase in the third that is in detail quite irregular. Ternary selenides are less well known but behave analogously in all respects as far as is known. Clearly there is some difficulty in any attempt to relate the net effect of all of these distances to the apparent degree of reduction of the cluster unless some procedure such as a bond order sum is employed.

A recent discussion of these bond distances (*6*) notes that the greater changes in the second Mo–Mo distance above (between the triangles) give some correlation with the amount of cluster reduction by *M*. However, this approach immediately runs into trouble in any comparison of sulfides with selenides with the same degree of reduction. As will become more evident when the nature of the matrix or steric effects in this structure type is considered, the third intercluster Mo–Mo distance necessarily depends on the radius of the nonmetal. Therefore, if a fixed amount of bonding (as expressed by bond orders) is to be found with a given number of cluster electrons, the diminished intercluster Mo–Mo bonding in the selenides *must* be reflected in shortened intracluster bonds. The good concordance of total Mo–Mo bonding in sulfides with selenides shown in Fig. 1 suggests that this view is correct. (Even if it is not, a different result *may* obtain for the selenides because of the significant and diverse nonbonding interactions which occur in these phases (*vide infra*).) But if attention is focused solely on the one intermediate intracluster distance and not on some measure of the total cluster bonding, the conclusion is made that the selenides are somehow more bonded than the sulfides. In order to account for this impression a rather unusual postulate was advanced (*6*), namely, that in all of the selenides 0.12–0.20 fewer electrons are actually transferred from metal to selenium than are necessary to give them a closed-shell configuration (filled valence band), thus leaving more for intracluster bonding. Or, in other words, the selenium

[4] Data for $Ni_{2.0}Mo_6S_8$ (*21*) have not been included as the nickel occupancy and distribution between sites was assumed rather than refined. However, the structural parameters are appropriate to a higher substitution level than in $Ni_{1.4}Mo_6S_8$.

but not the sulfur valence band was assumed to overlap the metal conduction band. A different approach which yields the same hypothesis has also been advanced based on van der Waals radii of the nonmetals (*23*). The net result seems artificial and unreasonable and in any case seems quite unnecessary when all the Mo–Mo distances and plausible nonbonding contacts are considered together.

The existence of a matrix effect in both the parent binary molybdenum chalcides Mo_6Ch_8 and the resultant Chevrel phases is strongly implied by the low bond orders of Fig. 1. This is based on the general observation (*1*) that in all other cases in which a reduced bond order is found one can discern a specific limitation on the close approach of metal atoms that is imposed by the nonmetal atoms. The same applies to the Chevrel phases as well but some unique features of the structure need to be considered in order that the source of the effect is clear. The bond order data for the isolated halide and mixed halide–chalcide clusters, $Mo_6S_6Cl_2$ especially, which so nicely group around 1.0 do make it clear that it is not an intracluster *Ch–Ch* repulsion which limits the approach of the metals to one another within Mo_6S_8 or Mo_6Se_8 clusters as they often do with the more crowded M_6X_{12} clusters. On the other hand, the intercluster Mo–*Ch* bonding turns out to be very strong and essentially structure determining.

Structural Differences

An important and fundamental difference between the Mo_6X_8 chalcide phases under consideration here and nearly all other 6-8 type clusters has to do with the source of the atoms which occupy the exo (also called *aussen, outer,* or *apical*) positions on the cluster. The nearest neighbor atoms to each Mo atom within a 6-8 cluster are four other Mo atoms on one side and four (inner) nonmetal atoms approximately coplanar with the central Mo atom. This leaves the part of the Mo coordination sphere which is outward from the cluster empty. A maxim of cluster chemistry is that these outer or exo positions are strongly bonding and are *always* occupied by some basic group. In all of the examples cited above in which PBO/*e* is close to 1.0 an extra basic molecule (H_2O, *Py*) or halide fulfills this role, either as a terminal ligand or bridging between clusters. Examples are $(Mo_6Cl_8^i)Cl_{4/2}^{a-a}Cl_2^a$,[5] $(PyH)_3(Mo_6Cl_7S)Cl_6^a$ and $(Mo_6Cl_7Se)Cl_{6/2}^a$. Exo positions in most niobium and tantalum 6-12 type cluster derivatives are found to be similarly occupied, but $(Nb_6Cl_{12})Cl_2$ is an exception more analogous to the molybdenum chalcides. Here there are insufficient halides outside of the cluster for bridging so that two of the inner halogens must also be exo to other clusters [i.e., $(Nb_6Cl_{10}Cl_{2/2}^{i-a})Cl_{2/2}^{a-i}Cl_{4/2}^{a-a}$] (*24*).

The molybdenum chalcides represent a stoichiometric extreme in this respect, lacking any extra nonmetal atoms whatsoever to occupy exo positions, but there is also reason from other structures to believe that Mo_6X_8-type clusters also bind atoms at these positions significantly more tightly than do Nb_6X_{12} types. The Mo–Cl distances involving exo, doubly bridging halide atoms (*a–a*) in Mo_6Cl_{12} and $Mo_6Cl_7SeCl_3$ are only 0.02 Å longer than those to the inner chlorides which bond to three metals and only cap faces, while those to halogens which are only terminal are 0.09 Å (Mo_6Cl_{12}) to 0.02 Å ($Mo_6Cl_7SCl_6^{3-}$) *shorter*. In contrast, the metal distances to bridging X^{a-a} atoms in 6-12 clusters are between 0.1 and 0.2 Å longer than to X^i atoms (Nb_6Cl_{14}, Ta_6Cl_{15}, $H_2Ta_6Cl_{18}\cdot 6H_2O$ (*24–26*)). In

[5] *i* = inner, *a* = outer terminal, *a–a* = outer bridging.

other 6-12 clusters where "double duty" inner halogen also occupies outer positions in other clusters the elongation of the inner $M-X$ bonds is small (0.06 Å, Nb_6Cl_{14}) to nil [$Sc(Sc_6Cl_{12})$ (*27*)] and the additional exo "bonds" formed are 0.2 to 0.5 Å longer. Perhaps the less favorable angles at face-capping nonmetal atoms in 6-8 type clusters result in less bonding (charge transfer) to the metal, or the electronic requirements at the exo positions in these are simply greater. In any case, the exo bonding in Mo_6X_8 clusters is significantly stronger, and this is evidently enhanced in the Mo_6Ch_8 chalcides by their higher oxidation states (lower electron count for metal–metal bonding) relative to that in the dihalides.

The extreme example presented by the binary and ternary chalcogenides is now clearer. The isostructural Mo_6S_8 and the Mo_6Se_8 as well as the Chevrel phases derived therefrom are unique in that the compounds lack any additional anions to occupy exo positions in the cluster. In the Lewis sense the phases are highly acidic. The compounds solve this by requiring that six of the eight chalcide atoms already each bound to three metals (type *Ch*1) also fill a fourth exo position in a neighboring cluster, and vice versa, a process which generates both a relatively short Mo–Mo intracluster distance and some of the evident matrix effects. The shortness and therefore presumably also the strength of this fourth intercluster Mo–S1 bond in Mo_6S_8 is especially remarkable; at 2.425 Å it is the same as the shortest of the three between that sulfur and the molybdenum atoms of the cluster face it caps, 2.426 Å (2.431 and 2.460 Å for the other two). The distances to the remaining two sulfur atoms in the cluster (S2, three coordinate) are the same as the average to S1 (2.439 Å). In the selenide (*28*) the intercluster Mo–Se1 distance is 0.03 Å longer than within the cluster while bonds to Se2 are 0.02 Å shorter than the others within the cluster.

Figure 2 shows two views, 90° apart, of a portion of the Mo_6S_8 structure (*22*). For clarity Fig. 2a shows only four of six clusters which bridge to each Mo_6S_8, while 2b illustrates all six clusters about the central one as viewed along the hexagonal c axis ($R\bar{3}$). For additional clarity only a partial set of sulfur atoms is shown on the outer clusters, namely, those which are necessary for bridging or important in nonbonding repulsions. A point of $\bar{3}$ symmetry occurs in the center of each cluster and at the origin (large M

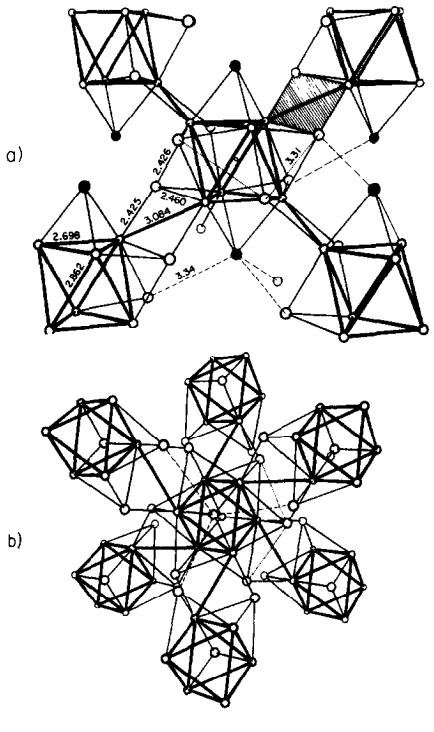

FIG. 2. Two views of Mo_6S_8 structure (*22*). (a) One complete central cluster with four (of six) adjoining clusters, c axis vertical, S2 atoms shaded. One short intracluster nonbonding contact is dotted, and one intercluster bridge is shaded. Only the S1 and S2 atoms on outer clusters which have important intercluster nonbonding distances (dashed) have been included. Arbitrary-sized thermal ellipsoids, (b) Same, down c axis.

site); two of the latter are marked with a small solid circle. An important feature of the structure are the rhomboids generated by two each of the short Mo–S1 intercluster and intracluster bonds, and these are bisected by the intercluster Mo–Mo bonds. One of these is shaded in the figure. There are six rhomboids giving 12 Mo–S1 and 6 Mo–Mo bonds between each cluster and its neighbors.

Nonbonding Repulsions and Matrix Effects

Past considerations of the obvious elongation of the molybdenum clusters in the binary chalcides and the somewhat regular reduction in this distortion which occurs on reduction with added *M* ions have usually attributed these results to "electronic effects." A more detailed examination of the crystal chemistry allows these to be understood much better. The reduced bond orders for the parent Mo_6S_8 and Mo_6Se_8 can be ascribed to a matrix effect from strong closed-shell repulsions which in turn originate at least in large part because of the unusually tight intercluster Mo–*Ch* bonding. Such effects give rise to a substantial elongation of the Mo_6 unit along the $\bar{3}$ axis, a distortion which diminishes but does not disappear on reduction, apparently in response mainly to lengthening of the exo Mo–*Ch* bonds. This is not to say that these complex structures can in any sense be completely understood. Their complex interconnectivity, the many and changing nonbonding contacts, and the role of the interstitial *M* atoms are difficult to analyze collectively and in any quantitative sense.

The nonmetal contacts which apparently require the elongation of the clusters in the first place are principally of the types *Ch*2–*Ch*1 between atoms in different clusters and *Ch*1–*Ch*1 within each cluster. What should be considered as a short *Ch*–*Ch* contact must be considered first. Obviously twice the conventional van der Waals radii for sulfur and selenium, ~3.7 and 4.0 Å, respectively (*2*), are inappropriately large since these are based only on the apparent sizes of S^{2-} and Se^{2-} in very polar salts. It is generally (but not always (*23*)) accepted that effective van der Waals radii of the more covalently bonded chalcogenides, as certainly pertains to these molybdenum compounds, will be less than the above values (as they are, for example, in Se_8^{2+} (*29*)). Suggestive values occur in the elements, where the shortest separations are apparently 3.45 Å in monoclinic sulfur (*30*) and 3.44 Å in trigonal selenium (*31*). However, these are apt to be anisotropic in character and data from other metal- (and electron-) rich chalcogenides are probably more appropriate sources and secondary bonding between the nonmetals is not likely to come into question. It has been noted before (*1*) that matrix effects in the metal-rich sulfides appear inevitable when one lattice dimension (and therefore the sulfur–sulfur repeat distances) fall as low as 3.32–3.36 Å. A similar effect occurs in selenides at ca. 3.44 Å. In particular, minimum *Ch*–*Ch* separations in the neighboring niobium chalcogenides seem to be the most appropriate references, 3.35 ± 0.01 Å in $Nb_{21}S_8$ and Nb_3S_4 and 3.42–3.45 Å in Nb_2Se and Nb_5Se_4 (and V_5Se_4) (*32*). These are somewhat less than twice the crystal radii which have been considered appropriate to "real" crystals, 3.40 and 3.68 Å, respectively (*33*), and presumably represent "tight" packing.

The shortest distances in Mo_6S_8 and Mo_6Se_8 are certainly significant by these standards. Two seem particularly important in the sulfide, 3.31 Å (×2) for S1–S1 across the waist within each cluster and 3.34 Å between each S2 atom and S1 atoms in three other clusters. Examples

of these are shown dotted and dashed, respectively, in Fig. 2. All other separations are ≥3.45 Å. In the selenide the intercluster (Se1–Se2) distances are relatively shorter, 3.38 Å (×3), but the first type within the cluster is a less significant 3.50 Å, these changes reflecting the larger size of selenium and the longer Mo–Se bonds, respectively. All other separations in Mo_6Se_8 are ≥3.58 Å. In these terms *the elongation of the Mo_6Ch_8 clusters is absolutely necessary*. Each end face of the molybdenum trigonal antiprism is tightly hinged to three other clusters beyond that face through 6 Mo–*Ch* (and 3 Mo–Mo) bonds, and it is this strong bonding which brings each *Ch*2 atom capping the face to within 3.34 (S) or 3.38 (Se) Å of *Ch*1 atoms lying across the waist of those same three clusters (see Fig. 2). Elongation of the cluster along the threefold axis appears the only possible alternative to lengthening the apparently strong intercluster bonds. In the sulfide this distortion can be considered to lead to the additional S1–S1 contacts at 3.31 Å around the waist of each cluster. The latter presumably further limit the cluster elongation in relief of nonbonding repulsions, and also imply something of the limited stability of the compound. In these terms there is nothing particularly unusual about the shorter Mo–Mo bonds (higher bond order) in Mo_6Se_8 relative to Mo_6S_8 (Fig. 1).

Reduction to Ternary Phases

The strong binding each Mo_6X_8 cluster to six neighbors and vice versa takes place through 12 short Mo–S linkages to each cluster. This combination generates a novel structure which (1) is strong yet somewhat flexible, (2) contains substantial amounts of free volume, and (3) exhibits a significant matrix effect (restricted Mo–Mo bonding). Evidences of these properties are provided in part by the structural changes which occur on reduction of the molybdenum cluster backbone with introduction of the heteroatom into the parent structure to form the so-called Chevrel phases $M_xMo_6Ch_8$. The larger *M* atoms are introduced at the origin (small solid dot in Fig. 2), while the smaller *M* atoms are according to the structure analysis displaced approximately laterally from these into two sets of six roughly tetrahedral interstices (see Yvon (*6*)). The response of the lattice parameters and distances to these *M* atoms will be seen to be rather diverse.

The openness and flexibility of the structure are fairly easy to perceive. Interstices of the small-*M* type of sufficient size to accommodate nickel are already present in Mo_6S_8 while the larger hole at the origin could contain a cation of radius ~0.69 Å in digonal coordination and with appreciably more space laterally (e.g., Li^+). That a far greater range of ion sizes can be accommodated because of the flexibility of the structure is demonstrated by the range of c/a ratios achieved in both sulfide and selenide. These values are plotted against the presumed additional degree of reduction (electrons added per cluster) in Fig. 3a.

The distinction between small-ion species (lower curve), where the host structure flattens on occupation of small ion sites, and large ion phases, in which the host elongates, is striking. (Indium and especially silver behave in an intermediate way and appear anomalous in many comparisons.) Nearly all of the lattices actually increase in volume during these substitutions so that the c/a function represents mainly the accompanying distortions. Those few cases in which the volume change is substantially less than expected apparently represent cases of strong binding by higher field ions and will be discussed later.

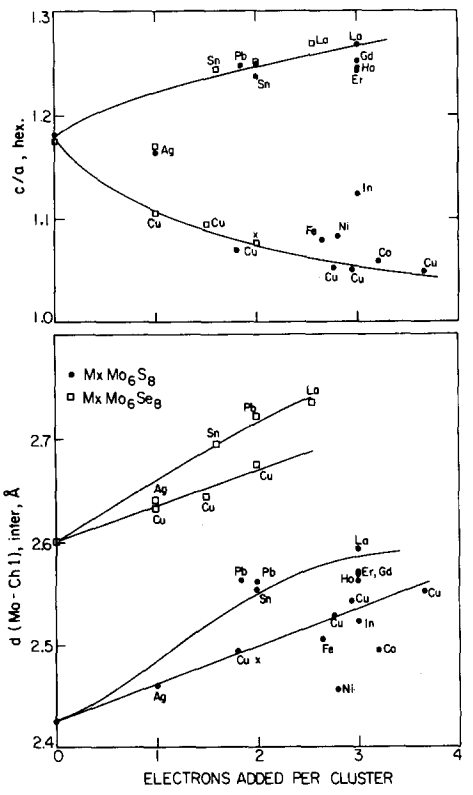

FIG. 3. (a) Hexagonal c/a parameters as a function of the number of electrons added to Mo_6Ch_8 cluster. Ch = S,●, or Se,□. (b) Intercluster or exo Mo–$Ch1$ bond length as a function of added electron count. (Small x refers to $Mo_6S_6Br_2$—see below.)

The magnitude of the change around the large metal site at the origin with changes in c/a is the easier to describe. The flattening of the structure with small ions, nickel for example, diminishes the origin–S_2 separation at the large hole by 0.34 Å from the value in the binary Mo_6S_8 (2.36 Å), while large ion La^{3+} is accommodated with an increase of 0.47 Å from the binary compound. Thus an increase in c/a of nearly 18% accompanies the change from nickel to lanthanum and with only a small change in electron count in the cluster. Small tetrahedral ion interstices of a size sufficient to contain Ni^{2+} are still present in the large-ion derivatives but these are probably all too close to the large M site to be sensibly occupied.

Superimposed on these flexings of the Mo_6Ch_8 substrate are a loosening of the structure on reduction through a significant (up to 0.17 Å) increase in the intercluster Mo–$Ch1$ (and therefore Mo–Mo) bonds, as shown in Fig. 3b. This relieves nonbonding repulsions and is accompanied by an 8.4% decrease in the height (parallel to the threefold axis) of the trigonal antiprism (a 5.4% decrease in the corresponding Mo–Mo bonds) as the geometry tends toward an octahedral configuration of the metal cluster on reduction. The decrease in Mo–Mo bonds just cited depends only slightly on the small vs large classification of the interstitial ion. Thus in the sulfides the exo Mo–$Ch1$ distances change from 2.42 Å in Mo_6S_8 to 2.55–2.59 Å with large M and ≥23 electrons (MCE ≥ 3.83), while at the same time the increase in the average intracluster Mo–S1 bonds is ≤0.04 Å and for the Mo–S2 distances in the capped faces, only 0.03–0.04 Å in the average (0.08 Å in the extreme). As with changes in most other parameters those for Mo–$Ch1$ intercluster distances characteristically split into separate groups, a more rapid increase for large-M atoms (larger c/a or smaller α) and a somewhat slower increase with small M (smaller c/a, large α). And the iron, cobalt, and nickel clusters are again out of place in that the amount of increase in the exo bond length is less than implied by the stoichiometry. Both of these aspects will be considered later. In the selenides the intercluster Mo–Se bonds similarly increase from 2.60 Å in Mo_6Se_8 to 2.73 Å in $La_{0.85}Mo_6Se_8$, while all Mo–Se capping distances vary only from 2.56 to 2.58 Å. Clearly the added electrons from M are particularly effective in screening or diminishing the bonding of nonmetal atoms in the outward pointing directions. Such an effect on reduction is not unique to

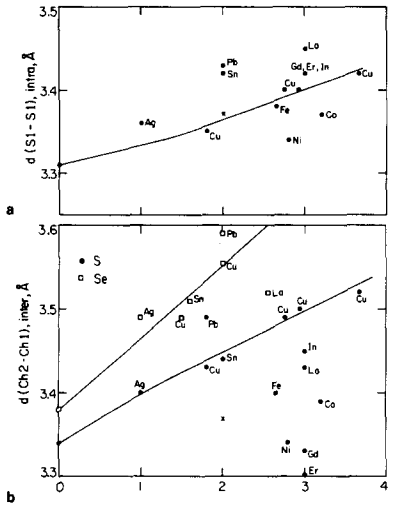

FIG. 4. (a) The shortest intracluster S1–S1 distances in $M_xMo_6S_8$ as a function of number of electrons added to the cluster by M. (b) Intercluster $Ch1$–$Ch2$ separations as a function of cluster reduction, Ch = S,●, or Se,□.

this system, however; a very similar increase in Nb-Cl^a distance (2.47 to 2.62 Å) is known to accompany the two-electron reduction of $Nb_6Cl_{12}Cl_6^{2-}$ to $Nb_6Cl_{12}Cl_6^{4-}$ (*34*).

The effect of reduction on the two kinds of close S–S contacts discussed earlier as regards the origin of the matrix effect is now easier to appreciate. As shown in Fig. 4a, the intracluster S1–S1 separation increases only moderately (3.40 ± 0.05 Å covering all phases, greatest with large-M ions), reflecting the flattening of the metal antiprism and only a slight increase in the length of the intracluster Mo–S1 bonds on reduction (0.04 Å over the range). The "nesting" contacts $Ch1-Ch2$, Fig. 4b, generally increase, more so for the seemingly more tightly packed Mo_6Se_8, but the changes are very uneven, the higher field ions actually achieving short and even shorter S1–S2 contacts irrespective of c/a. (The implied tighter binding of the structure by these ions will be considered later.) And other S–S distances now become significantly short during reduction with large M because of both the increase in c/a and the tight binding, 3.42–3.45 Å for three more S2–S1 contacts between clusters (3.51–3.54 Å for Sn, Pb, and La selenides) and 3.38–3.41 Å in intercluster S1–S1 distances with the heavier rare earths. Some insight into the seemingly diverse reaction of especially the S1–S2 distances to reduction will be presented shortly.

The end result on reduction, the distribution of the effect of these diverse closed-shell repulsions together with the increased binding of the cluster among the three types of Mo–Mo bonds is clearly complex, and the rate of increase of the PBO/e likewise (Fig. 1). The structures for the low-field copper(I) phases, where there are short nonbinding contacts only around the waist of each cluster, may represent closer to the optimal configurations at the bridge. The net leveling which is manifested in a relatively smooth increase in the net PBO/e on reduction is still remarkable, as is the fact that the selenide results are so similar to those for the sulfides.

This increase in effective Mo–Mo bonding on reduction will be seen to be just the opposite to that expected for simple "first principle" systems. Ordinarily electrons added to a partially filled manifold of bonding levels would occupy higher energy orbitals of lesser bonding capability, and the effect per electron would decrease. The dominance of a strong matrix effect clearly overwhelms the expectation for a simpler system.

Some effects of the binding forces in these phases can be seen in changes in the intercluster bonding, especially in the rhomboids which are generated by pairs of Mo–Ch intercluster bonds and which contain the intercluster Mo–Mo bonds. These figures remain substantially planar and only flatten or extend more or less along c in response to changes in c/a.

Small twists of the Mo_3 triangles also occur, 1.6° in the extreme, probably because of stronger binding by the interstitial ions, especially the heavier rare earths. However, this change can be better seen in the angle defined by the center of the cluster (C), a neighboring molybdenum atom vertex and the exo bridging atom opposite ($C-Mo-Ch1b$). The sulfide data are shown in Fig. 5a. Deviations of this from 180° measure the displacement of the exo atom from what is usually taken to be the optimum exo position, more or less equidistant from four adjacent sulfurs on the same cluster.

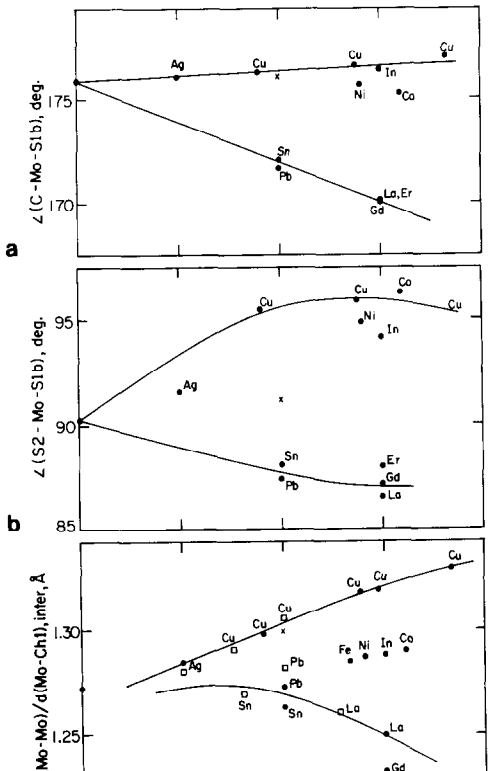

FIG. 5. Structural parameters in $M_xMo_6Ch_8$ as a function of the number of electrons added to the cluster by M. (a) The angle (cluster center C–Mo–S1 (exo or bridging) in $M_xMo_6S_8$. (b) The angle S2–Mo–S1 (bridging). (c) The distance ratio Mo–Mo/Mo–$Ch1$ (exo) in the intercluster bridge.

For the sulfide phases the only significant change from an angle of ~176° is seen to occur again with the large-M substituents as c/a increases. The selenide function is quite similar for a more limited set of compounds, starting at 173° and spreading to 175.3° (Cu_2) and 169.8° ($La_{0.85}$). It seems plausible that the somewhat more rapid increase in the length of the cluster Mo–Ch bonds with the larger-M ions, Fig. 3b, results from a bond weakening associated with greater deviation of this exo bond from the ideal. The deviations seen for Fe, Co, Ni in Fig. 3b presumably arise from a more fundamental problem, a loss of charge from and weakening of the bonding in the cluster, as will be discussed later.

Another parameter graphically reflects the swinging of the intercluster bridge planes and behaves very much like, but inversely to, c/a. This is the more acute angle from $Ch2$, the unshared capping atom on the threefold axis, through a neighboring Mo to its exo bridging $Ch1b$ from another cluster. This behavior is shown in Fig. 5b for the sulfides. (Compare c/a, Fig. 3a). The change seen here is somewhat accentuated by changes in capping S2–Mo distances which also vary in a similar way (see below). The selenide behavior is very parallel to that shown, starting at 88.6° because of the longer Mo–Se2 bonds.

The twist accompanying large changes in c/a is easily seen in the shape of the bridge rhomboids. One of the easier representations to come by is shown in Fig. 5c, the ratio of the intercluster bridge distances Mo–Mo to Mo–$Ch1$, two edges of a nearly isosceles triangle closely related to the angle at the molybdenum in the bridge. This angle (~102°) opens up with small M atoms (by ≤6°) and closes down (≤3.3°) with the largest ions, the Fe, Co, Ni, In problems being intermediate. The intercluster Mo–Mo distance itself always increases on reduction as Mo–$Ch1$

(bridge) lengthens and the metal cluster becomes more nearly regular and more strongly bonded, with the least changes (again) with the dipositive 3*d* metals and the heavier rare earths.

Though the changes in nonbonding repulsions between chalcogenide atoms during reduction with various *M* atoms is complex, these effects remain even after the addition of nearly four electrons per cluster, basically because of the framework structure of the host. That this must be true is shown by the striking *increase* in amount of metal–metal bonding achieved with even more (26) cluster electrons and more Mo–Mo bonds in the infinite chains of confacial octahedra in $^{1}_{\infty}(Mo_6Se_8^{2-})$, Fig. 1. The structure now allows full realization of the Mo–Mo bonding potential as the minimum Se–Se distances are now 3.76 Å. The exo bond to nonmetal at each molybdenum is now replaced by pairs of edge-bridging chalcogenide atoms around and coplanar with the equilateral triangles of metal which comprise the shared faces.

Iron, Cobalt, and Nickel Phases

The behavior of these sulfides appears anomalous not only with respect to bond orders (Fig. 1) but also in many other structural dimensions (e.g., Figs. 3a, 4b, 5c). The small-ion Chevrel phases for which refined positional parameters are available for the rhombohedral cell are limited to only these three plus the copper(I) sulfides and selenides. The crystal structure analysis indicated that the added metal in these is disordered over two sets of sixfold distorted tetrahedral interstices. The anomalously low bond order sum for the Mo–Mo bonds in the iron, cobalt, and nickel sulfides were calculated on the basis of the only reasonable assumption regarding oxidation states, the transfer of two electrons per *M* atom to the cluster matrix. The shorter *M*–S distances in the Fe, Co, Ni, Cu phases are all reasonable for the assigned oxidation states based on provisional sulfide radii (*35*); 2.24–2.37 Å for the first three in site one, 2.19–2.35 Å in the less occupied site two, and 2.28–2.42 Å in $Cu_{3.66}Mo_6S_8$. These are also similar to those found in other phases, e.g., Ni_3S_2 (2.25, 2.28 Å), γ-NiS (3 at 2.24 Å) (*36*) and Cu_2S (2.28–2.32 Å) (*37*). But a most striking feature which does not appear to have been discussed before are the remarkably short *M*–Mo distances indicated by the structures for these small atoms, increasing in number and decreasing in length from Cu: 3.07, 3.13 Å, Fe: 3.01 (×2) Å, Co: 3.02, 3.04, 3.09 Å to Ni: 2.97, 3.01 and 3.07 (×2) Å. All but the last distance for Ni occur only with *M* atoms in type two positions, and all other *M*–Mo distances for the dipositive examples are >3.50 Å.

A quantitative judgment regarding these short distances is difficult to achieve, but for the purposes of comparison it will simply be assumed that the bond order for a heterometal separation can similarly be judged from the Pauling equation (1) using the sum of the appropriate single bond metallic radii. For the 3d elements these are, computed as before, Fe: 1.183, Co: 1.162, Ni: 1.154, and Cu: 0.954 Å (ν = 1). With R_1 for Mo of 1.310 Å these yield bond orders of 0.14 to 0.09 for each of the Fe, Co, Ni distances cited and ≤0.05 for all of those to copper. Those for Fe, Co, and Ni are in the right order and aggregate to more than enough to account for the bond order discrepancies seen in Fig. 1. Of course the numbers should not be taken too literally, for there is no good evidence that the tail of the bond order function utilized is very accurate at such distances. But the distances and the Mo–Mo bond orders for all of the Chevrel phases are certainly consistent with a significant transfer of charge and electrons from the cluster to *only* the nearer and higher field Fe, Co, and Ni

atoms (but not the diamagnetic Cu^+). Magnetic properties of the first three should be appreciably affected; they have been found not to be superconducting. Single-crystal data for the corresponding Fe, Co, Ni selenides are not available but the postulated M–Mo bonding should, if correctly assigned, be less because the corresponding nonmetal interstices will probably be further removed from the cluster with the larger selenide.

In connection with the structure of the small ion phases it is worth noting that the indicated low fractional occupancies of the $M(1)$ and $M(2)$ sites, e.g., 13 and 10% in $Ni_{1.4}Mo_6S_8$, respectively, would if correctly interpreted be necessary because of the many short M–M distances which would otherwise result. For example, there are seven different nickel site separations between 1.27 and 2.30 Å ($2R_1$). At low loading these sites are presumably randomly occupied so as to avoid filling adjacent sites. The occurrence of a recognizable superlattice with the rhombohedral $Ni_{1.4}Mo_6S_8$ phase (*38*) may be a manifestation of ordering of the light atoms. Only four Cu–Cu distances in the sulfide phases are less than $2R_1$ because of the larger lattice dimensions, but similar effects seem likely at high loading.

Radii and Binding of M Atoms

The probable presence of significant amounts of covalent and coulombic binding in different examples of the Chevrel phases can be judged from radii comparisons together with changes in c/a ratios and other parameters already presented. Except for the rare earth elements the M–S bonds represented would generally be considered as rather covalent. It is interesting to note that, with the same exceptions, the M elements involved are geochemically classified as chalcophilic, that is, sulfide as opposed to oxygen (silicate) seeking (*39*). And the observed M–S distances with the small ions are quite consistent with a recent set of sulfide-based radii (*35*). But the digonal coordination found at the large M site (with six additional neighbors ≥0.2 Å more distant) is virtually unknown for the rare earth ions although it does occur in a few sulfides of elements such as Sn and Ag. Notwithstanding, the M–$Ch2$ separations in the rare earth metal phases are described quite well by the sum of the standard (*33*) crystal radii. Figure 6 compares the observed M–$Ch2$ distances for large M with the crystal radius sum for coordination number six (1.23 Å was estimated for Sn(II)). An empirical reduction of the sum by 0.06 Å describes the M–S2 separations in the less covalent rare earth metal phases very well, and the La–Se relationship is also satisfactory when the 85% occupancy is allowed for. Some of this agreement is probably accidental; presumably a reduction in cation radius would occur on reduction to two coordination, but polarization (and size reduction) of the sulfur by the three molybdenum atoms to which is is also bonded certainly must also be a part of the result.

More significant are the impressively smaller M–Ch separations found in the Sn, Pb, and especially the Ag phases relative to standard six-coordinate crystal

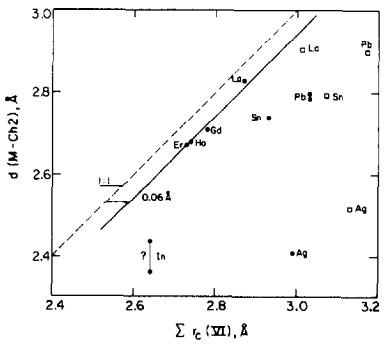

FIG. 6. Observed M–$Ch2$ distances (Å) for large M in $M_xMo_6Ch_8$ vs the sum of six-coordinate crystal radii (from (*33*)) ●,S; □,Se.

radii (which have been deduced largely from oxide and fluoride structures). These decreases appear to be typical examples of the effect of reduced coordination and of "covalent shortening" (*33*). The bonding in many tin(II) and lead(II) compounds is characteristically covalent (*37*) and, as will be shown, the behavior of silver is even more extreme. Still the distances observed in these phases are quite consistent with those found in other sulfides (*35*). The observed Sn–S separation of 2.74 Å compares well with 2.79 Å recently deduced for two-coordinate tin in $SnTaS_2$ (*40*) while it is somewhat larger than the nearest neighbors in SnS and Sn_2S_3 (2.62–2.74 Å for four-coordinate Sn) (*37*). The observed distance in $PbMo_6S_8$, 2.78 Å, compares favorably with 2.73 Å for the three-coordinate lead in $PbN_2S_2 \cdot NH_3$ (*37*). And $AgMo_6S_8$, which shows the greatest deviation from the ideal or ionic radii of silver, by ca. 0.6 Å, is actually behaving quite typically by sulfide standards. The observed Ag–S distance, 2.41 Å (2.43 Å if displaced 0.3 Å off the axis as suggested by its thermal ellipsoid (*41*)), compares very well with separations for two-coordinate silver found in both AgSCN, 2.43 Å, and $(Ag_3S)NO_3$, 2.41 and 2.55 Å (*37*). And it is the $AgMo_6Ch_8$ phases which also show otherwise inexplicable deviations in many other parameters previously examined, most particularly the low c/a ratios (Fig. 3a), where it is seemingly misassigned as a "large ion." In fact the silver phases are the only ones in which the size of the molybdenum face bonded to *Ch*2 actually increases in dimensions relative to that in Mo_6S_8 and Mo_6Se_8 (by 0.005 and 0.039 Å, respectively), implying that this covalency polarization also affects the cluster bonding and lowers the Mo–Mo bonding (Fig. 1). (Perhaps silver lies below E_F in this state.)

Indium presents several problems. Although the six-coordinate radius for indium(III) used in the figure is too large, the sum of four-coordinate radii (2.46 Å) is only 0.02–0.10 Å larger than observed. The largest of the distances shown in the figure is based on the observed partial displacement of the indium from the large hole toward the small ion site, as suggested by abnormal size of the thermal ellipsoid normal to c (*41*). That notwithstanding, the In^{3+} ion, which is only ca. 0.1 Å larger than four-coordinate Fe^{2+} and Cu^{2+} (sulfide radii (*35*)), still remains 0.25–0.30 Å further removed from the S1 atoms which would complete a tetrahedron than it is from S2. A "large-ion" description might therefore seem better but in some structural parameters the phase tends to group with the small ion results. Indium(III) probably represents the lower size limit for a "large" ion, thereby actually reducing c/a. Significant covalence would be expected chemically for this element and oxidation state and is suggested by Fig. 6. Assumption of indium(I) in the Chevrel sulfide would cause many of the structural parameters considered to fit much better with those of other phases but not with respect to bond orders; however, the indium(I) ion appears to be 0.7–0.8 Å larger than indium(III) (based on the shorter distances found in the chlorides (*42*)) and as such would not fit. Photoelectron spectroscopic data for this phase could be a useful confirmation of the oxidation state assignment. This applies even more so to the less well defined $InMo_6Se_8$ recently reported (*43*), especially in view of the relatively large In–Se distance cited (without error limit) (compare also In_4Se_3 (*44*) and $Rb_6In_2S_6$ (*45*)).

An interesting alternate explanation comes to mind regarding the apparent partial (25–50%) delocalization of the silver and indium from the large ion hole toward the six inner tetrahedral sites. This might be considered to represent an approach to a lattice instability (*41*) or,

alternatively, to arise from a compression by the tightly bridged binary host. But it is at the very least a remarkable coincidence that the angle at silver in the $Ag_3S(NO_3)$ and AgSCN compounds cited above, 157° and ~165°, respectively, are so close to the 166° value calculated for the estimated lateral 0.30 Å displacement of Ag from the origin in $AgMo_6S_8$ and $AgMo_6Se_8$. Perhaps these displacements really represent a preference for certain bond angles in covalent bonding in cases with low coordination, i.e., ~152° for In, aided perhaps by compression by the matrix, whereas the behavior of Cu, Ni, etc. represent a more conventional, three- or four-coordinate limit for smaller ions.

Volume and Constriction Effects

A definite constriction of the Mo_6S_8 matrix when lanthanum is substituted by the heavier rare earth metal ions is explicit in several of the structural parameters. Most impressive is its effect on the hexagonal cell volume relative to expectation based on the volume of the parent Mo_6S_8 phase plus that of the added ion according to crystal radii. The ratio V_{obs}/V_{calc} for the sulfides is shown in Fig. 7, using four-coordinate sulfide radii (*35*) for the small ions, Ag and In and six for the remainder (*33*). In effect the covalent shortening with the former group is now included and what remains is any additional constriction. The dashed line approximates the result if the added ions were ~75% effective in filling space, that is, approximately close packed. The ions which have the higher charges or polarization, namely Gd, Er, Ho, Co, and Ni appear to provide a definite constriction of the cell, although the behavior regarding Co and Ni is clouded by their apparently significant interactions with molybdenum discussed earlier. Parallel effects with the heavier rare earth metal ions are seen in angles in and to the bridge and the exo position (Fig. 5) and, most particularly, in the shortest intercluster S1–S2 distances which evidently restrict the approach of clusters and generate the matrix effect, Fig. 4. A significant and presumably coulombic contribution to the binding in phases containing the rare earth metals seems clear. Sulfide phases containing the nominal U^{4+}, Th^{4+}, and Y^{3+} also show this constriction judging from their molar volumes (*6*) and ion sizes. On the other hand, the copper phases have been suggested to involve only weak binding by the interstitial metal (*41*), and this seems consistent with their volumes and the cluster parameters. These effects are less marked in the smaller collection of selenides.

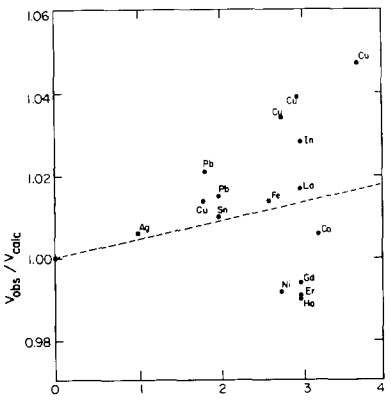

FIG. 7. Ratio of observed hexagonal cell volume of $M_xMo_6S_8$ to volume calculated for Mo_6S_8 plus $3 \times M$ vs number of electrons added to the cluster by M.

A recent study shows that densities of $Cu_xMo_6S_8$ phases clearly extrapolate to a value for Mo_6S_8 about 2% higher than the experimental density (*46*). This is consistent with the present analysis in terms of a sizable matrix effect from nonmetal repulsions. In particular, the very short intracluster S1–S1 distance of 3.31 Å which evidently limits compression of the metal antiprism appears similarly out of line, since extrapolation of these data for the $Cu_xMo_6S_8$ phases, Fig. 4a, gives an expectation value ~0.02 Å smaller. This is not a limiting factor in the selenides.

In contrast to the behavior with copper, the introduction of large and higher charged metal ions such as the rare earth elements forces an elongation in c/a but with an increased Madelung contribution to stability in return. The Mo–*Ch*2 distances, Fig. 8, show an unusual trend which can be interpreted as reflecting the increased binding. Ordinarily one would expect a slight increase in the Mo–*Ch*2 distance as the cluster is further reduced and the metal cores become better screened, as occurs with *d*(Mo–*Ch*1). (Although introduction of a large *M* atom increases the coordination number of *Ch*2 this has a negligible effect on the radius of sulfur (*35*).) But what is actually seen, Fig. 8, is a diminished Mo–*Ch*2 distance with large ions. An obvious explanation is that the compression applied by the matrix in response to introduction of large *M* atoms and an increased coulombic interaction actually shorten the Mo–*Ch*2 distances.

Delk and Sienko (*47*) have observed that a rather good correlation exists between T_c and c/a ratios for Chevrel phases containing the rare earth elements. Not surprisingly, a number of other parameters in these structures also vary as does c/a, viz., the angle S2–Mo–S1 (bridge) and the Mo–S1 bridge, S1–S1 intracluster, and the Mo–S2 distances just considered. In fact the Mo–*Ch*2 distances (Fig. 8) provide one of the better variables in paralleling T_c for large ions, though the comparison is greatly limited by the availability of single-crystal data. According to the above analysis this distance reflects something of the tightness of packing and strain in the c direction owing to both the nature of the host structure and a coulombic contribution. Delk and Sienko considered the c/a ratio in a similar way but viewed an increase in that parameter in the opposite way as reflecting a weakening of interactions out c.

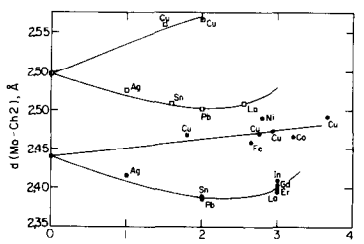

FIG. 8. The Mo–*Ch*2 distances in $M_xMo_6Ch_8$ as a function of the number of electrons added per cluster.

Good structural data for large-ion phases with Sr, Ba, Sc (?), Sm, Eu, U, Tl, etc. would help clarify these aspects of the crystal chemistry in the region where high T_c occurs and then is lost. And data on other phases containing smaller ions, e.g., Li, Zn, Cd, Al, Ga (?) would doubtlessly improve the understanding of those structures.

Other Phases

Some related compounds offer considerable support for the ideas developed earlier, especially as regards the origin and behavior of the matrix effect in the Mo_6Ch_8 host.

$Mo_6S_6Br_2$. Substitution of the larger bromine into the unique S2 position on the threefold axis give a more reduced (22-electron) cluster which exhibits a substantially reduced c/a ratio (*28*). The structural parameters are very much like those of the copper sulfide phases at the same degree of reduction and are marked with a small x in Figs. 3, 4, 5a, and 5c. Although S1–S1 contacts about the waist of the cluster are fairly typical for copper at that electron count, the short *Ch*2–*Ch*1 intercluster contacts, which forced cluster elongation in other phases (Fig. 2), are now very much in effect with the larger bromine and in effect require a low c/a ratio. The distance of 3.37 Å for Br–S1 compares with an average of ca. 3.40 Å for distances judged earlier as "tight" in other phases and about 3.5 Å as a reasonable expectation for a "normal"

mixed bromine–sulfur contact based on Fig. 4b. The consequence of such a relatively short Br–S1 contact is in accord with earlier discussions, a greater distortion of the cluster and a greater matrix effect. This exhibits itself in a PBO/e value of 0.75 for the ideal stoichiometry (MCE = 3.67) (or 0.76 for the reported bromine deficiency, $Mo_6S_6(Br_{1.77}S_{0.23})$). But in this case it is the shortest Mo–Mo distance in the cluster which is enlarged, that within, not between, the Mo_3 triangles, presumably in response to the more lateral effect of the large bromine. The increase is 0.04 Å relative to the Sn, Pb and $Cu_{1.8}Mo_6S_8$ and $Cu_2Mo_6Se_8$ and 0.02 Å with respect to Mo_6S_8 itself. In this case the cluster comes much closer to octahedral symmetry.

Substitution of small ions in this phase should be possible, a change which has been accomplished in $Cu_xMo_6S_6I_2$ (*49*). A new range of "large" ions at the origin does not seem likely inasmuch as the Br–Br separation is only 3.91 Å and the contact distance would be about 3.5 Å.

Mixed clusters. Two recent examples have been well described structurally, $(In^+)_2[(Mo_6Se_8)(Mo_9Se_{11})]^{2-}$ (*50*) and $(Tl^+)_4[(Mo_6S_8)(Mo_{12}S_{14})]^{4-}$ (*51*). The 9- and 12-atom molybdenum clusters represent intermediate degrees of cluster condensation between the discrete Mo_6Ch_8 examples and the infinite chains $^1_\infty(Mo_3Ch_3^-)$ and behave accordingly with respect to bond orders. The intercluster connectivity in these two phases is comparable to that in the simpler binary and ternary systems already considered; the exo positions at Mo (but only those in the end triangles in the Mo_9 and Mo_{12} groups) are filled by chalcogenide atoms from the other type of cluster, and vice versa, thereby again generating long intercluster Mo–Mo bonds, and the intercluster interactions and nonbonding repulsions fulfill a similar role. The important intra- and intercluster Se–Se interactions in the Mo_6Se_8 group at 3.55 and 3.59 Å are comparable to those in $Cu_2Mo_6Se_8$, and the cluster is elongated much as it is in $AgMo_6Se_8$. In the more reduced sulfide the equivalent of the S1–S1 intracluster contacts at 3.40 Å (misprinted in (*51*)) plus intercluster S-S contacts at 3.44, 3.45, and 3.48 Å (3 each) are all significant, and the Mo_6S_8 cluster is elongated about midway between that found in $AgMo_6S_8$ and $Cu_{1.8}Mo_6S_8$. On the other hand, the middle portions of the Mo_9 and Mo_{12} clusters involve increasingly fewer nonmetal repulsions (Ch–$Ch \geq$ 3.47, 3.67 Å, respectively) and the metal atoms there are accordingly more tightly bound. Although there is no way to assign charges to the individual clusters and thereby to calculate bond orders for each cluster the probable limits show the same results:

Mo_6Se_8:	charge 0 to −2,	PBO/e = 0.81 − 0.74	0.84 net,
Mo_9Se_{11}:	charge −2 to 0,	PBO/e = 0.85 − 0.90	
Mo_6S_8:	charge 0 to −2,	PBO/e = 0.81 − 0.73	0.89 net.
$Mo_{12}S_{14}$:	charge −4 to −2,	PBO/e = 0.92 − 0.96	

Even in these ranges the results are in accord with expectations—the Mo_6Ch_8 groups show a significant loss of bonding because of the indicated matrix effects and give typical PBO/e values in the range of 0.73–0.81. In the actual compound this is averaged with larger and increasing PBO/e values of 0.85–0.96 for the less hindered and better bonded Mo_9 or Mo_{12} unit. Thus the overall averages of

0.84 and 0.89 for MCE values of 3.60 and 3.78, respectively, are significantly above those for the remainder of the Chevrel phases in Fig. 1. The less well-defined clusters in $In_{\sim 3}(Mo_6Se_8)(Mo_9Se_{11})$ (*52*) give quantities which are roughly comparable to those in the above selenide. In bond order terms there is certainly no evidence for Mo–Mo antibonding effects accompanying cluster condensation, as has been claimed (*43*), rather just the opposite as antibonding effects arising from the *non*metal diminish.

A rhenium cluster. A 6-8 cluster of rhenium has been described which appears quite analogous to that in the molybdenum sulfides, viz., in $Na_4Re_6S_{12}$ (*53*). The cluster and its connectivity are described as $[(Re_6S_8)S^a_{4/2}(S^a_2)_{2/2}]^{4-}$. Since there are extra sulfide and disulfide groups to bridge between the 6-8 clusters, a matrix-free result should be found, and bond order calculations support this expectation completely. The question of how many valence electrons are involved for rhenium must be considered first. Conventional wisdom describes the above cluster as a 24-electron $Re_6S_8^{2+}$, isoelectronic with that in $Mo_6Cl_8Cl_4$. In effect this assumes all seven valence electrons of the element are involved. If D_1 for the metal is calculated on the same basis (2.610 Å) the Pauling bond order in $Na_4Re_6S_{12}$ is a very satisfying 0.99. Comparable bond order results are also obtained from data recently reported for $K_4Re_6S_{12}$ as well as for the sodium phase (*54*).

Acknowledgments

The author is particularly indebted to R. Chevrel, M. Sergent, R. E. McCarley and R. D. Shannon for structural details in advance of publication and to R. N. Shelton and J.-L. Staudenmann for helpful comments regarding the manuscript.

References

1. J. D. CORBETT, *J. Solid State Chem.* **37**, 335 (1981).
2. L. PAULING, "The Nature of the Chemical Bond," 3rd ed., pp. 400, 403. Cornell Univ. Press, Ithaca, N.Y. (1960).
3. E. TEATUM, J. WABER, AND K. GSCHNEIDNER, quoted by W. B. PEARSON, "The Crystal Chemistry and Physics of Metals and Alloys," p. 151. Wiley–Interscience, New York (1972).
4. H.-G. VON SCHNERING, private communication (1978).
5. R. CHEVREL, M. SERGENT, AND J. PRIGENT, *J. Solid State Chem.* **3**, 515 (1971).
6. K. YVON, "Current Topics in Material Science" (E. Kaldis, Ed.), Vol. 3, p. 83. North-Holland, Amsterdam (1979).
7. Ø. FISCHER, *Appl. Phys.* **16**, 1 (1978).
8. H.-G. VON SCHNERING, *Z. Anorg. Allg. Chem.* **385**, 75 (1971).
9. J. B. MICHEL AND R. E. MCCARLEY, to be published.
10. C. PERRIN, M. SERGENT, F. LE TRAON, AND A. LE TRAON, *J. Solid State Chem.* **25**, 197 (1978).
11. K. JÖDDEN, H.-G. VON SCHNERING, AND H. SCHÄFER, *Angew. Chem.* **87**, 594 (1975).
12. M. POTEL, R. CHEVREL, AND M. SERGENT, *Acta Crystallogr. Sect. B* **36**, 1545 (1980).
13. W. HÖNLE, H.-G. VON SCHNERING, A. LIPKA, AND K. YVON, *J. Less-Common Metals* **71**, 135 (1980).
14. L. J. GUGGENBERGER AND A. W. SLEIGHT, *Inorg. Chem.* **8**, 2041 (1969).
15. R. SIEPMAN, H.-G. VON SCHNERING, AND H. SCHÄFER, *Angew. Chem.* **79**, 650 (1967).
16. J. C. WILDERVANCK AND F. JELLINEK, *Z. Anorg. Allg. Chem.* **328**, 309 (1964).
17. A. SIMON, *Z. Anorg. Allg. Chem.* **355**, 311 (1967).
18. H. IMOTO AND J. D. CORBETT, *Inorg. Chem.* **19**, 1241 (1980).
19. R. E. MCCARLEY, "Mixed Valence Compounds" (D. B. Brown, Ed.), p. 337, Reidel, Dordrecht (1980).
20. K. YVON AND A. PAOLI, *Solid State Commun.* **24**, 41 (1977).
21. J. GUILLEVIC, O. BARS, AND D. GRANDJEAN, *J. Solid State Chem.* **7**, 158 (1973).
22. R. CHEVREL, M. SERGENT, AND J. PRIGENT, *Mater. Res. Bull.* **9**, 1487 (1974).
23. M. SERGENT, Ø. FISCHER, M. DECROUX, C. PERRIN, AND R. CHEVREL, *J. Solid State Chem.* **22**, 87 (1977).
24. A. SIMON, H.-G. VON SCHNERING, H. WÖHRLE, AND H. SCHÄFER, *Z. Anorg. Allg. Chem.* **339**, 155 (1965).
25. D. BAUER AND H.-G. VON SCHNERING, *Z. Anorg. Allg. Chem.* **361**, 259 (1968).
26. C. B. THAXTON AND R. A. JACOBSON, *Inorg. Chem.* **10**, 1460 (1971).

27. J. D. CORBETT, R. L. DAAKE, K. R. POEPPELMEIER, AND D. H. GUTHRIE, *J. Amer. Chem. Soc.* **100**, 652 (1978).
28. O. BARS, J. GUILLEVIC, AND D. GRANDJEAN, *J. Solid State Chem.* **6**, 48 (1973).
29. R. K. MCMULLAN, D. J. PRINCE, AND J. D. CORBETT, *Inorg. Chem.* **10**, 1749 (1971).
30. Y. WATANABE, *Acta Crystallogr. Sect. B* **30**, 1396 (1974).
31. P. CHERIN AND P. UNGER, *Inorg. Chem.* **6**, 1589 (1967).
32. H. F. FRANZEN, *Progr. Solid State Chem.* **12**, 1 (1978).
33. R. D. SHANNON, *Acta Crystallogr. Sect. A* **32**, 751 (1976).
34. F. W. KOKNAT AND R. E. MCCARLEY, *Inorg. Chem.* **13**, 295 (1974).
35. R. D. SHANNON, *in* "Structure and Bonding in Crystals" (M. O'Keefe and A. Navrotsky, Eds.), Vol. II. Academic Press, New York, in press.
36. "Gmelin's Handbuch der Anorganische Chemie," 8th ed., No. 57, Teil B2, pp. 634, 657. Springer-Verlag: Berlin Heidelberg (1966).
37. A. F. WELLS, "Structural Inorganic Chemistry," 4th ed., pp. 616, 747, 908, 937. Claredon, Oxford (1975).
38. R. CHEVREL AND M. SERGENT, Private communication (1980).
39. V. M. GOLDSCHMIDT, *J. Chem. Soc.*, 655 (1937).
40. R. EPPINGA AND G. A. WIEGERS, *Mater. Res. Bull.* **12**, 1057 (1977).
41. K. YVON, *Solid State Commun.* **25**, 327 (1978).
42. G. MEYER, private communication (1980).
43. A. LIPKA AND K. YVON, *Acta Crystallogr. Sect. B* **36**, 2123 (1980).
44. J. H. C. HOGG, H. H. SUTHERLAND, AND D. J. WILLIAMS, *Acta Crystallogr. Sect. B* **29**, 1590 (1973).
45. H.-J. DEISEROTH, *Z. Naturforsch. B* **35**, 953 (1980).
46. R. FLÜKIGER, R. BAILLIF, J. MULLER, AND K. YVON, *J. Less-Common Metals* **72**, 193 (1980).
47. F. S. DELK AND M. J. SIENKO, *Solid State Commun.* **31**, 699 (1979).
48. C. PERRIN, R. CHEVREL, M. SERGENT, AND Ø. FISCHER, *Mater. Res. Bull.* **14**, 1505 (1979).
49. F. J. CULETTO AND F. POBELL, *Mater. Res. Bull.* **14**, 473 (1979).
50. M. POTEL, R. CHEVREL, AND M. SERGENT, *Acta Crystallogr.* (in press).
51. M. POTEL, R. CHEVREL, AND M. SERGENT, *Acta Crystallogr. Sect B* **36**, 1319 (1980).
52. A. GRÜTTNER, K. YVON, R. CHEVREL, M. POTEL, M. SERGENT, AND B. SEEBER, *Acta Crystallogr. Sect. B* **35**, 285 (1979).
53. S. CHEN AND W. R. ROBINSON, *J. Chem. Soc., Chem. Commun.*, 879 (1978).
54. W. BRONGER AND M. SPANGENBERG, *J. Less-Common Metals* **76**, 73 (1980).